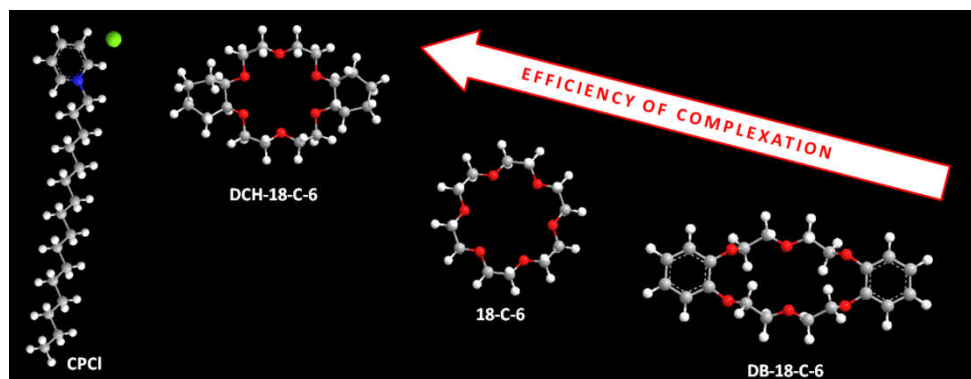


CHAPTER IX

Probing supramolecular complexation of cetylpyridinium chloride with crown ethers

Supramolecular complexations of cetylpyridinium chloride with three comparable cavity dimension based crown ethers, namely, dibenzo-18-crown-6, 18-crown-6 and dicyclohexano-18-crown-6 have been explored and adequately compared in acetonitrile with the help of conductivity in a series of temperatures to reveal the stoichiometry of the three host-guest complexes. Programme based mathematical treatment of the conductivity data affords association constants for complexations from which the thermodynamic parameters were derived for better comprehension about the process. The interactions at molecular level have been explained and decisively discussed by means of FT-IR and ^1H NMR spectroscopic studies that demonstrate H-bond type interactions as the primarily force of attraction for the investigated supramolecular complexations.



IX.1. Introduction

Crown ethers (CEs) are used as important hosts in supramolecular chemistry, where the host-guest interaction mimics natural systems as well as constructs various materials.[1-6] CE are macromolecular heterocyclic compounds with essential repeating unit $-\text{CH}_2\text{CH}_2\text{O}-$. [7] A number of researchers are working on fabrication of crown-ether-based stimuli-responsive materials that have unique characters of ion recognize ability.[8-10] A variety of current supramolecular materials, for instance rotaxanes are made on

these unique recognition properties of CEs.[11,12] Binding of CEs with cations with high selectivity and affinity has found remarkable importance in chemistry.[13,14] Formation of molecular assemblies has vast implication for the building of molecular machines having plausible use as analogous to sophisticated machines of natural systems.[15,16] Hence, fundamental investigations of the interactions between CEs and cationic species are important for their advanced applications.[17,18] In the present work cetylpyridinium chloride (CPCI) (scheme 1) has been investigated as the cationic species, which is structurally significant because of having long lipophilic chain and pyridinium cationic head and also has medicinal applications, while three CEs, namely, dibenzo-18-crown-6 (DB-18-C-6), 18-crown-6 (18-C-6) and dicyclohexano-18-crown-6 (DCH-18-C-6) (scheme 2) have been selected with similar cavity dimension, but having different and tailored abilities to construct supramolecular complexes.[19-23] The complexation processes have been explored in CH₃CN solution with definite host-guest type interactions in molecular level.[24,25] Pyridinium based ionic liquids (ILs) are biologically extremely significant and also have role in material chemistry for their extraordinary properties.[26-28] Here, the structure of CPCI is very important to make supramolecular materials and also has biological and medicinal functions.[29,30] In this study the three complexation processes require special attention to explore the various interactions taking place in molecular level.[31,32] Conductivity measurement and programmed mathematical treatment of the data offer quantitative idea about association constant and thermodynamic parameters, whereas FT-IR and ¹H NMR spectroscopic studies deliver specific information about the complexation processes for the potential applications in supramolecular host-guest chemistry.

IX.2. Experimental section

IX.2.1. Source and purity of samples

Cetylpyridinium chloride, dibenzo-18-crown-6, 18-crown-6 and dicyclohexano-18-crown-6 of puriss grade have been bought from Sigma-Aldrich, Germany and used as received. Purity of cetylpyridinium chloride, dibenzo-18-crown-6, 18-crown-6 and dicyclohexano-18-crown-6 were ≥98.0%, ≥98.0%, ≥99.0% and ≥98.0% respectively.

IX.2.2. Apparatus and procedure

Solubilities of cetylpyridinium chloride, dibenzo-18-crown-6, 18-crown-6 and dicyclohexano-18-crown-6 have been verified in HPLC grade CH₃CN. All the stock solutions of CPCI and crown ethers were arranged by mass using Mettler Toledo AG-285 with uncertainty ± 0.1 mg. Sufficient precautions were made to minimize the evaporation during mixing and working with these solutions.

Specific conductivity values of the experimental solutions were measured by Mettler Toledo Seven Multi conductivity meter with uncertainty $\pm 1.0 \mu\text{S m}^{-1}$. The measurements were carried out using HPLC grade CH₃CN in an auto-thermostat water bath maintaining at ± 0.1 K of the desired temperature. The cell was calibrated using standard procedure.

Fourier transform infrared (FT-IR) spectra were recorded on a Perkin Elmer FT-IR spectrometer in CH₃CN solution. The FTIR measurements were performed in the scanning range of 4000–400 cm⁻¹ at room temperature.

¹H NMR spectra were recorded in CD₃CN at 300 MHz using Bruker Avance 300 MHz instrument at 298 K. Signals are cited as δ values in ppm using residual protonated solvent signal as internal standard (CH₃CN, δ 1.96 ppm). Data are reported as chemical shift.

IX.3. Results and discussion

IX.3.1. Conductivity study

Conductivity study is a convincing method for exploring complexation in solution not only because it affords information for minute alteration of concentrations of the charged particles, but also it offers data for the various interactions among the particles taking place in the solution system.[33,34] Conductivity of a solution with IL and added CE provides valuable information for the complexation process between the CE and IL in solution.[35,36] In our work complexations have been explored between CPCI and three similar CEs in CH₃CN solution. Thus to acquire data about complexation, conductivity of the CPCI solution with initial concentration of 10.0 mM have been measured with increasing concentration of the three CEs at five various temperatures from 293 K to 313 K in 5 K intervals and presented in [table 1-3](#) with increasing CE/IL mole ratio. The plots of

conductance are depicted in [figure 1-3](#), in which CE/IL mole ratio is shown in abscissa and conductance is shown in ordinate. A gradual decrease in conductance is observed with increasing CE/IL mole ratio for each plot, which signifies capture of the cetylpyridinium ions by the CEs respectively in CH₃CN solution, because CPCI being strong electrolyte can't form ion pair in the studied solution system.[\[37\]](#) So the complexation processes of cetylpyridinium ion with the three CEs which have been illustrated by decrease in conductance in [figure 1-3](#), become approximately plateau as the CE/IL mole ratio exceed 1.0, evidently suggesting development of adequately stable 1:1 CPCI-CE complex in CH₃CN solution system.[\[38\]](#) Each of the figures ([figure 1-3](#)) shows five various curve at different temperatures, all exhibiting analogous variation in conductance. At elevated temperatures the conductances become high because of enhanced mobility of the cetylpyridinium ions, as a result of lowered viscosity of CH₃CN solution.[\[39\]](#)

IX.3.2. Association constants and thermodynamic parameters

Association constants (K_a) for the formation of complexes have been derived by a mathematical programme based on non-linear changes in conductance for 1:1 CPCI-CE complexation at various temperatures.[\[37-39\]](#)

The following equilibrium is supposed to exist between CPCI and CE during complexation.



Thus K_a for the complex (CX) may be illustrated as

$$K_a = \frac{[\text{CX}]}{[\text{CPCI}]_f[\text{CE}]_f} \quad (\text{IX.2})$$

Here, [CX], [CPCI]_f and [CE]_f correspond to the equilibrium concentration of CX, free CPCI and free CE respectively.

In accordance with the non-linear isotherm the K_a for the CX may be illustrated as [\[36,39\]](#)

$$K_a = \frac{[\text{CX}]}{[\text{CPCI}]_f[\text{CE}]_f} = \frac{(\kappa_{obs} - \kappa_o)}{(\kappa - \kappa_{obs})[\text{CE}]_f} \quad (\text{IX.3})$$

where,

$$[\text{CE}]_f = [\text{CE}]_{ad} - \frac{[\text{CPCI}]_{ad}(\kappa_{obs} - \kappa_o)}{(\kappa - \kappa_o)} \quad (\text{IX.4})$$

Here, κ_o , κ_{obs} and κ are conductivities of CPCI at initial state, during addition of CE and final state respectively. $[\text{CPCI}]_{ad}$ and $[\text{CE}]_{ad}$ are concentrations of CPCI and the added CE respectively.

Hence K_a for complexation processes have been evaluated from various isotherms by using mathematical programme and presented in [table 4](#), which illustrates different values of K_a for each of the three complexes at the experimental temperature range, may be because of higher thermal agitation of the ions at increased temperatures that lowers the values of K_a with rise in temperature.[\[40,41\]](#) It is also noted from [table 4](#) that CPCI has binding efficiency to form the complexes with the three studied CEs in the order of DB-18-C-6 < 18-C-6 < DCH-18-C-6 in CH_3CN solution.

The thermodynamic parameters furnish comprehensive idea about the complexation processes taking place in solution.[\[39\]](#) The changes in standard enthalpy (ΔH°), entropy (ΔS°) and free energy (ΔG°) during complexation are fundamental factors for this process.[\[40,41\]](#) ΔH° is essentially responsible for the cetylpyridinium ion-CE interactions, higher solvation of the complex in CH_3CN , decreased repulsion among the adjacent donor oxygen atoms, relaxed conformations of the CEs after complexation and formation of H-bonds between aromatic hydrogen of CPCI and oxygen atoms of CEs. ΔS° is primarily accountable for the decrease in number of free species after complexation and conformational constraints of CEs associated with complex formation. Hence, for better understanding of the complexations that is to estimate the thermodynamic parameters van't Hoff equation was used as follows [\[40\]](#)

$$\ln K_a = -\frac{\Delta H^\circ}{RT} + \frac{\Delta S^\circ}{R} \quad (\text{IX.5})$$

According to [equation IX.5](#), $\ln K_a$ vs $1/T$ was plotted for each of the three complexes to obtain ΔH° and ΔS° from slope and intercept of the curves respectively ([figure 4](#)). Subsequent values of ΔG° have been derived from following equation at 298 K.

$$\Delta G^\circ = \Delta H^\circ - T\Delta S^\circ \quad (\text{IX.6})$$

The values of ΔH° , ΔS° and ΔG° for the complexations are presented in [table 4](#), which demonstrates negative values for all three parameters. The attraction between CPCI and CEs in CH_3CN are attributed to the negative enthalpy change while union of CPCI and CEs is accountable for negative entropy change during complexation processes. Thus, favorable changes in ΔG° are driven by higher negative value of ΔH° that play the key role for the spontaneity of all three complexation processes.[\[42,43\]](#)

IX.3.3. Infrared spectroscopic study

Infrared spectroscopy is a useful technique to identify complexation in solution system.[\[44,45\]](#) In this work the FT-IR spectra were taken in CH_3CN solution in 4000–400 cm^{-1} range. [Figure 5](#) demonstrates the FT-IR spectra of DB-18-C-6, CPCI and the complex, where the particular interactions between CPCI and DB-18-C-6 can be detected. In [table 5](#) it is observed that the stretching frequency of $(\text{C}^{\text{sp}^3}\text{-O})_{\text{str}}$ of free DB-18-C-6 is 1128 cm^{-1} , in the complexed state $(\text{C}^{\text{sp}^3}\text{-O})_{\text{str}}$ is 1115 cm^{-1} that generates frequency shift of 13 cm^{-1} and the stretching frequency of $(\text{C}^{\text{sp}^2}\text{-O})_{\text{str}}$ at free state is 1252 cm^{-1} , in complexed state $(\text{C}^{\text{sp}^2}\text{-O})_{\text{str}}$ is 1241 cm^{-1} that produces frequency shift of 11 cm^{-1} . These shifts signify participation of oxygen atoms of DB-18-C-6 in complexation, but it is also observed that the oxygen atoms linked to benzene ring have lower shift than those which are linked to methylene group. Alternatively, $(\text{C}^{\text{sp}^2}\text{-H})_{\text{str}}$ of CPCI has free and complexed stretching frequencies at 3012, 2926, 2854 cm^{-1} and 3002, 2920, 2850 cm^{-1} respectively producing shifts of 10, 6, 4 cm^{-1} . These information not only point out that pyridinium ring hydrogen atoms of CPCI are concerned in the interaction with the oxygen atoms of DB-18-C-6 making H-bond type involvement, but also that the oxygen atoms linked to benzene ring have weaker interaction with CPCI than those which are linked to methylene group.[\[45,46\]](#)

The FT-IR spectra of 18-C-6, CPCI and the complex are presented in [figure 6](#), that also specify the specific interactions of CPCI with 18-C-6 molecule. The frequency of $(\text{C-O})_{\text{str}}$ of 18-C-6 in free state is 1110 cm^{-1} and in complexed state is 1096 cm^{-1} , making a shift of 14 cm^{-1} ([table 5](#)), denoting again the oxygen atoms of the cyclic-ether are associated in complexation with the IL. $(\text{C}^{\text{sp}^2}\text{-H})_{\text{str}}$ of CPCI have stretching frequencies at 3012, 2926, 2854 cm^{-1} and 3000, 2918, 2848 cm^{-1} in the free and complexed states respectively

generating frequency shifts of 12, 8, 6 cm^{-1} in that order. These data again support that pyridinium ring hydrogen atoms are involved in the particular interaction with the oxygen atoms of 18-C-6 making H-bonds between them.[46,47]

The complexation of DCH-18-C-6 with CPCI has also been studied by FT-IR spectroscopy and shown in figure 7. Here, for the CE, frequencies of $(\text{C}^{1^\circ}-\text{O})_{\text{str}}$ are 1098 cm^{-1} (free state) and 1085 cm^{-1} (complexed state) and the frequencies of $(\text{C}^{2^\circ}-\text{O})_{\text{str}}$ are 1060 cm^{-1} (free state) and 1042 cm^{-1} (complexed state), making frequency shifts of 13 cm^{-1} and 18 cm^{-1} respectively (table 5). $(\text{C}^{\text{sp}2}-\text{H})_{\text{str}}$ of CPCI have stretching frequencies at 3012, 2926, 2854 cm^{-1} and 2998, 2917, 2846 cm^{-1} in the free and complexed states respectively causing frequency shifts of 14, 9, 8 cm^{-1} correspondingly. These shifts signify participation of oxygen atoms of DCH-18-C-6 in complexation, but it is also observed that the oxygen atoms linked to 2° carbon of cyclohexyl group have higher shift than those which are linked to methylene group. These information again not only point out that pyridinium ring hydrogen atoms of CPCI are concerned in the interaction with the oxygen atoms of DCH-18-C-6 making H-bond type involvement, but also that the oxygen atoms linked to 2° carbon of cyclohexyl group have stronger interaction with CPCI than those which are linked to methylene group.[45-47]

One more interesting comparison is observed from the FT-IR study that the frequency shifts of the $(\text{C}^{\text{sp}2}-\text{H})_{\text{str}}$ of CPCI for the three complexation processes are in the order of DB-18-C-6 < 18-C-6 < DCH-18-C-6, which is highly in agreement with the results found from the mathematical treatment of conductivity data, that is the association constants of the three complexes have similar order as found from the order on interactions in FT-IR study.

IX.3.4. ^1H NMR spectroscopic study

The complexations of CPCI with the three CEs, namely, DB-18-C-6, 18-C-6 and DCH-18-C-6 have been explored by ^1H NMR spectroscopy in CH_3CN solution at 298 K. Figure 8-10 show ^1H NMR spectra of the three complexes of CPCI with DB-18-C-6, 18-C-6 and DCH-18-C-6 respectively. Detailed and marked spectra of DB-18-C-6, CPCI and the complex are

illustrated in [figure 8](#), which describes slight downfield shift of the aliphatic protons of CE (free CE $\delta = 3.86-3.89$ ppm for $H_2C-O-CH_2$, 4.10-4.13 ppm for arom- $O-CH_2$ and complexed CE $\delta = 3.88-3.91$ ppm for $H_2C-O-CH_2$, 4.11-4.14 ppm for arom- $O-CH_2$ respectively) with nearly unshifted signal of the aryl protons and little broadening with slight upfield shift of the protons of pyridinium ring (free CPCI $\delta = 8.18-8.22$, 8.66-8.68, 8.89-8.91 ppm and complexed CPCI $\delta = 8.17-8.21$, 8.65-8.67, 8.88-8.90 ppm respectively) with almost unshifted signal of the cetyl group ([table 6](#)). This result evidently reveals existence of some kind of association between the electron rich oxygen atoms of DB-18-C-6 and the electron deficient protons of pyridinium ring, may be of H-bond type in CH_3CN solution, signifying as the key factor for the complexation process.[\[48-50\]](#)

In [figure 9](#) marked 1H NMR spectra of 18-C-6, CPCI and the complex are presented, that also demonstrate broadening with upfield shift of the pyridinium ring protons (free CPCI $\delta = 8.18-8.22$, 8.66-8.68, 8.89-8.91 ppm and complexed CPCI $\delta = 8.17-8.21$, 8.64-8.66, 8.87-8.89 ppm respectively) with nearly unshifted signal of the cetyl group and small downfield shift of the protons of CE (free CE $\delta = 3.55$ ppm, complexed CE $\delta = 3.59$ ppm respectively) ([table 6](#)). These spectral data also support the union of the electron deficient hydrogen atoms of pyridinium ring and electron rich oxygen atoms of 18-C-6 to form the complex.[\[41,48\]](#)

1H NMR spectra of DCH-18-C-6, CPCI and the complex are demonstrated in [figure 10](#), which explain downfield shift of the protons of CE (free CE $\delta = 3.59-3.61$ ppm for $-O-CH_2$ & $-O-CH$ and complexed CE $\delta = 3.64-3.66$ ppm for $-O-CH_2$ & $-O-CH$ respectively) with practically unshifted signals of the cyclohexyl $-CH_2-$ protons and broadening with upfield shift of the protons of pyridinium ring (free CPCI $\delta = 8.18-8.22$, 8.66-8.68, 8.89-8.91 ppm and complexed CPCI $\delta = 8.16-8.20$, 8.63-8.65, 8.86-8.88 ppm respectively) with approximately unshifted signal of the cetyl group ([table 6](#)). These findings obviously state the presence of H-bond like association between the electron rich oxygen atoms at DCH-18-C-6 and the electron deficient protons at pyridinium ring in CH_3CN solution.[\[48,49\]](#)

The CPCI-CE attraction in CH_3CN medium is the outcome of the presence of electron deficient and electron rich species respectively in the non-polar medium.[\[50,51\]](#) Dielectric

constant of acetonitrile is low, thus ionic or dipolar species in this medium can approach sufficiently close to interact with each other making the CPCI-CE complexes mainly through H-bond type interaction between electron deficient ring protons of pyridinium and electron rich oxygen atoms of CEs, thus lowering the enthalpy as well as entropy of the system.[41-43]

In DB-18-C-6 + CPCI complex the oxygen atoms which are attached to benzene ring are less effective donor compared to the oxygen atoms which are linked to alkyl group, thus overall electron donating ability of DB-18-C-6 is less compared to 18-C-6, in which electron delocalization through benzene ring is not possible.[52] On the other hand in DCH-18-C-6 + CPCI complex the electron donating ability of the oxygen atoms is enhanced by positive inductive effect of cyclohexyl groups, thus here CPCI-CE interaction is highest.[53,54] This fact is reflected in the extent of ^1H NMR signal shifts of pyridinium ring protons as well as CE protons and in the association constant values of the three complexes, which inform that, the order of feasibility of complexation is $\text{DCH-18-C-6 + CPCI} > \text{18-C-6 + CPCI} > \text{DB-18-C-6 + CPCI}$. [54,55]

IX.4. Conclusion

This study emphasize to the definite interactions between cetylpyridinium chloride and three similar macrocyclic polyethers toward complexation in acetonitrile in a range of temperature. Here, conductivity measurement helps to ascertain the association of CPCI with the three CEs in 1:1 stoichiometry, whereas the programmed mathematical treatment reveals quantitative data for complexation processes. Thermodynamic parameters have also been estimated for better perceptive about the complexations. The detailed interactions in molecular level have been elucidated by FT-IR and ^1H NMR spectroscopy that explains dipolar attractions due to H-bonding is the major operating force in the three complexes. During complexation the entropy of the system is decreased, but lowering of enthalpy has greater effect that makes the complexation spontaneous. This study not only presents remarkable information about supramolecular complexation of CPCI with the three analogous CEs, but also suggests admirable comparison among the studied CEs for construction of various types of CE-IL host-guest materials.

Tables

Table 1. Conductivity of mole ratio of DB-18-Crown-6/CPI at various temperatures

Mole Ratio (CE/IL)	κ /mS m ^{-1a}				
	293 K ^a	298 K ^a	303 K ^a	308 K ^a	313 K ^a
0.0	112.1	115.4	118.9	123.0	126.9
0.1	107.4	110.6	114.5	118.4	122.5
0.2	102.8	106.0	109.8	114.0	118.1
0.3	98.0	101.7	105.6	109.6	113.6
0.4	93.2	97.0	101.0	104.9	109.2
0.5	88.9	92.7	96.6	100.6	104.7
0.6	84.2	88.0	91.9	95.9	100.0
0.7	80.3	84.1	88.0	92.0	96.1
0.8	76.6	80.4	84.3	88.3	92.4
0.9	73.1	76.9	80.8	84.8	88.9
1.0	69.8	73.6	77.5	81.5	85.6
1.1	68.0	71.8	75.7	79.7	83.8
1.2	67.1	70.9	74.8	78.8	82.9
1.3	66.5	70.3	74.2	78.2	82.3
1.4	66.1	69.9	73.7	77.8	81.9
1.5	65.6	69.4	73.3	77.3	81.4
1.6	65.1	68.9	72.8	76.8	80.9
1.7	64.7	68.5	72.4	76.4	80.5
1.8	64.3	68.1	72.0	76.0	80.1
1.9	63.8	67.6	71.5	75.5	79.6
2.0	63.4	67.2	71.1	75.1	79.2

^a Standard uncertainties (*u*): temperature: $u(T) = \pm 0.01$ K, conductivity: $u(\kappa) = \pm 0.1$ mS·m⁻¹.

Table 2. Conductivity of mole ratio of 18-Crown-6/CPI at various temperatures

Mole Ratio (CE/IL)	κ /mS m ^{-1a}				
	293 K ^a	298 K ^a	303 K ^a	308 K ^a	313 K ^a
0.0	110.9	115.0	118.9	123.0	126.9
0.1	103.8	108.0	111.8	115.9	120.0
0.2	97.7	101.8	105.7	109.8	113.7
0.3	92.3	96.4	100.3	104.4	108.3
0.4	86.5	90.6	94.5	98.7	102.7
0.5	82.1	86.2	90.1	94.3	98.1
0.6	77.5	81.6	85.5	89.6	93.5

0.7	73.6	77.7	81.6	85.7	89.6
0.8	69.9	74.0	77.9	82.0	85.9
0.9	66.4	70.5	74.4	78.5	82.4
1.0	63.1	67.3	71.1	75.3	79.2
1.1	61.3	65.4	69.3	73.4	77.3
1.2	60.4	64.5	68.4	72.5	76.4
1.3	59.8	63.8	67.8	71.9	75.8
1.4	59.4	63.4	67.4	71.4	75.4
1.5	58.9	62.9	66.9	71.0	74.9
1.6	58.4	62.5	66.5	70.5	74.4
1.7	58.0	62.1	66.0	70.1	74.0
1.8	57.6	61.7	65.6	69.7	73.6
1.9	57.1	61.2	65.2	69.2	73.1
2.0	56.7	60.8	64.8	68.8	72.7

^a Standard uncertainties (*u*): temperature: $u(T) = \pm 0.01$ K, conductivity: $u(\kappa) = \pm 0.1$ mS·m⁻¹.

Table 3. Conductivity of mole ratio of DCH-18-Crown-6/CPCl at various temperatures

Mole Ratio (CE/IL)	κ /mS m ^{-1a}				
	293 K ^a	298 K ^a	303 K ^a	308 K ^a	313 K ^a
0.0	109.7	113.8	117.8	122.0	125.8
0.1	99.8	104.0	108.2	112.5	116.6
0.2	91.6	95.6	99.6	103.5	108.0
0.3	85.3	89.0	92.9	96.7	101.2
0.4	79.9	83.4	87.5	91.1	95.5
0.5	75.4	79.1	82.8	86.8	90.8
0.6	70.7	74.4	78.2	82.1	86.1
0.7	66.8	70.5	74.3	78.2	82.2
0.8	63.1	66.8	70.6	74.5	78.5
0.9	59.6	63.3	67.1	71.0	74.8
1.0	56.3	60.0	63.8	67.7	71.7
1.1	54.5	58.2	62.0	65.9	69.9
1.2	53.6	57.3	61.1	65.0	69.0
1.3	52.9	56.7	60.5	64.4	68.4
1.4	52.5	56.3	60.0	64.0	68.0
1.5	52.1	55.8	59.6	63.5	67.5
1.6	51.6	55.3	59.1	63.0	67.0
1.7	51.2	54.9	58.7	62.6	66.6
1.8	50.8	54.5	58.3	62.2	66.2
1.9	50.3	54.0	57.8	61.7	65.7
2.0	49.9	53.6	57.4	61.3	65.3

^a Standard uncertainties (*u*): temperature: $u(T) = \pm 0.01$ K, conductivity: $u(\kappa) = \pm 0.1$ mS·m⁻¹.

Table 4. Association constant, enthalpy, entropy and Gibbs energy change for various CE-IL complexes in CH₃CN at different temperatures

	K _a					ΔH° /kJ mol ^{-1b}	ΔS° /J mol ⁻¹ K ^{-1b}	ΔG° /kJ mol ^{-1b} (at 298 K)
	/M ^{-1b}							
	293 K ^a	298 K ^a	303 K ^a	308 K ^a	313 K ^a			
DB-18-crown-6	83	77	72	66	61	-11.73	-3.26	-10.76
18-crown-6	149	136	124	114	105	-13.37	-4.03	-12.17
DCH-18-crown-6	199	179	165	149	136	-14.41	-5.16	-12.87

^a Standard uncertainties in temperature u are: $u(T) = \pm 0.01$ K.

^b Mean errors in $K_a = \pm 1$ M⁻¹; $\Delta H^\circ = \pm 0.01$ kJ mol⁻¹; $\Delta S^\circ = \pm 0.01$ J mol⁻¹K⁻¹; $\Delta G^\circ = \pm 0.01$ kJ mol⁻¹.

Table 5. Change in frequencies at FTIR spectra for various CE-IL complexes in CH₃CN at room temperature

DB-18-Crown-6 + CPCI complex			
Group	Free state / cm ^{-1a}	Complexed state / cm ^{-1a}	Shift / cm ^{-1a}
(C ^{sp3} -O) _{str} of CE	1128	1115	13
(C ^{sp2} -O) _{str} of CE	1252	1241	11
(C ^{sp2} -H) _{str} of IL	3012, 2926, 2854	3002, 2920, 2850	10, 6, 4
18-Crown-6 + CPCI complex			
Group	Free state / cm ^{-1a}	Complexed state / cm ^{-1a}	Shift / cm ^{-1a}
(C-O) _{str} of CE	1110	1096	14
(C ^{sp2} -H) _{str} of IL	3012, 2926, 2854	3000, 2918, 2848	12, 8, 6
DCH-18-Crown-6 + CPCI complex			
Group	Free state / cm ^{-1a}	Complexed state / cm ^{-1a}	Shift / cm ^{-1a}
(C ^{1°} -O) _{str} of CE	1098	1085	13

$(C^{2^{\circ}}-O)_{\text{str}}$ of CE	1060	1042	18
$(C^{\text{sp}2}-H)_{\text{str}}$ of IL	3012, 2926, 2854	2998, 2917, 2846	14, 9, 8

^a Spectral resolution = 0.5 cm⁻¹.

Table 6. ¹H NMR data of DB-18-C-6, 18-C-6, DCH-18-C-6, CPCI and various CE-IL complexes in CH₃CN

DB-18-C-6 (300 MHz, Solv: CD ₃ CN)	
δ /ppm	
3.86-3.89 (8H, m, H ₂ C-O-CH ₂), 4.10-4.13 (8H, m, arom-O-CH ₂), 6.89-6.96 (8H, m, aryl)	
18-C-6 (300 MHz, Solv: CD ₃ CN)	
δ /ppm	
3.55 (24H, s, OCH ₂)	
DCH-18-C-6 (300 MHz, Solv: CD ₃ CN)	
δ /ppm	
1.23 (4H, m), 1.41 (8H, m), 1.71 (4H, m), 3.59-3.61 (20H, m, -O-CH ₂ & -O-CH)	
CPCI (300 MHz, Solv: CD ₃ CN)	
δ /ppm	
0.78-0.82 (3H, t, J = 6.5 Hz), 1.38-1.44 (28H, m), 4.67-4.71 (2H, t, J = 6.6 Hz), 8.18-8.22 (2H, m), 8.66-8.68 (1H, m), 8.89-8.91 (2H, m)	
DB-18-C-6 +CPCI complex (300 MHz, Solv: CD ₃ CN)	
δ /ppm	
0.78-0.82 (3H, t, J = 6.5 Hz), 1.38-1.44 (28H, m), 3.88-3.91 (8H, m, H ₂ C-O-CH ₂), 4.11-4.14 (8H, m, arom-O-CH ₂), 4.67-4.71 (2H, t, J = 6.6 Hz), 6.89-6.96 (8H, m, aryl), 8.17-8.21 (2H, m), 8.65-8.67 (1H, m), 8.88-8.90 (2H, m)	
18-C-6 +CPCI complex (300 MHz, Solv: CD ₃ CN)	
δ /ppm	
0.78-0.82 (3H, t, J = 6.5 Hz), 1.38-1.44 (28H, m), 3.59 (24H, s, OCH ₂), 4.67-4.71 (2H, t, J = 6.6 Hz), 8.17-8.21 (2H, m), 8.64-8.66 (1H, m), 8.87-8.89 (2H, m)	
DCH-18-C-6 +CPCI complex (300 MHz, Solv: CD ₃ CN)	

δ /ppm
0.78-0.82 (3H, t, $J = 6.5$ Hz), 1.23 (4H, m), 1.38-1.45 (36H, m), 1.71 (4H, m), 3.64-3.66 (20H, m, -O-CH ₂ & -O-CH), 4.67-4.71 (2H, t, $J = 6.6$ Hz), 8.16-8.20 (2H, m), 8.63-8.65 (1H, m), 8.86-8.88 (2H, m)

Figures

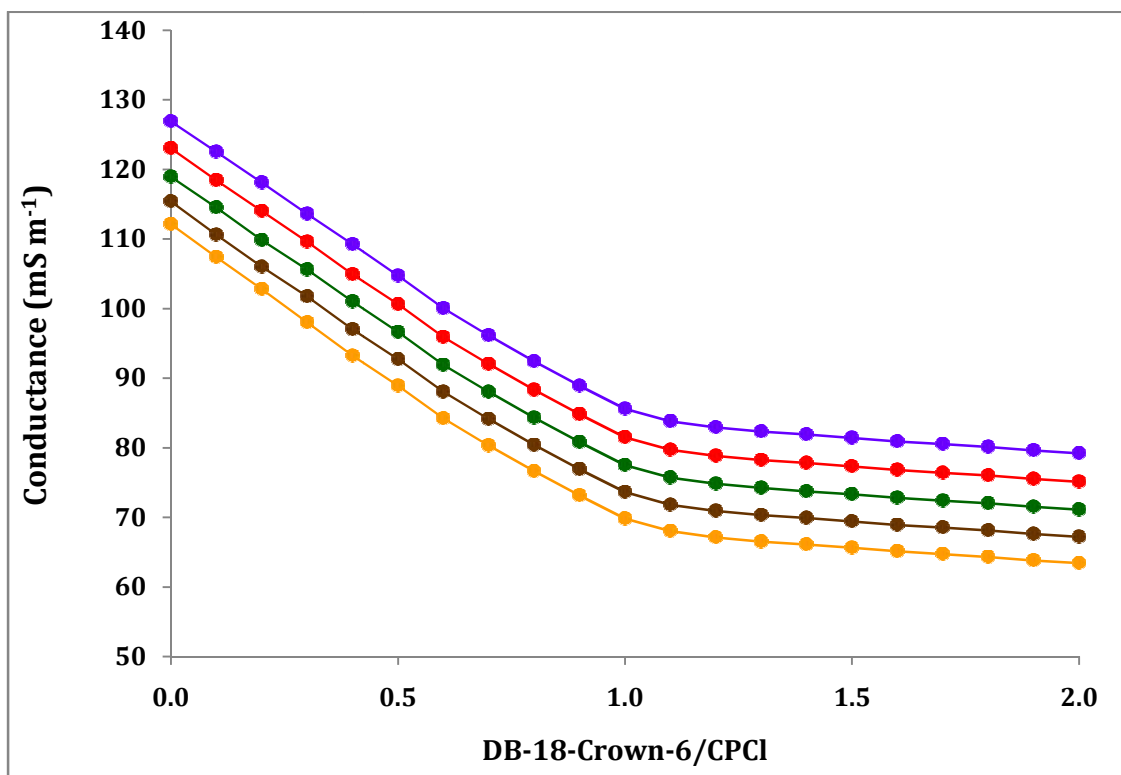


Figure 1. Variation of conductance of DB-18-crown-6/CPCl mole ratio at different temperatures (● 293 K, ● 298 K, ● 303 K, ● 308 K, ● 313 K).

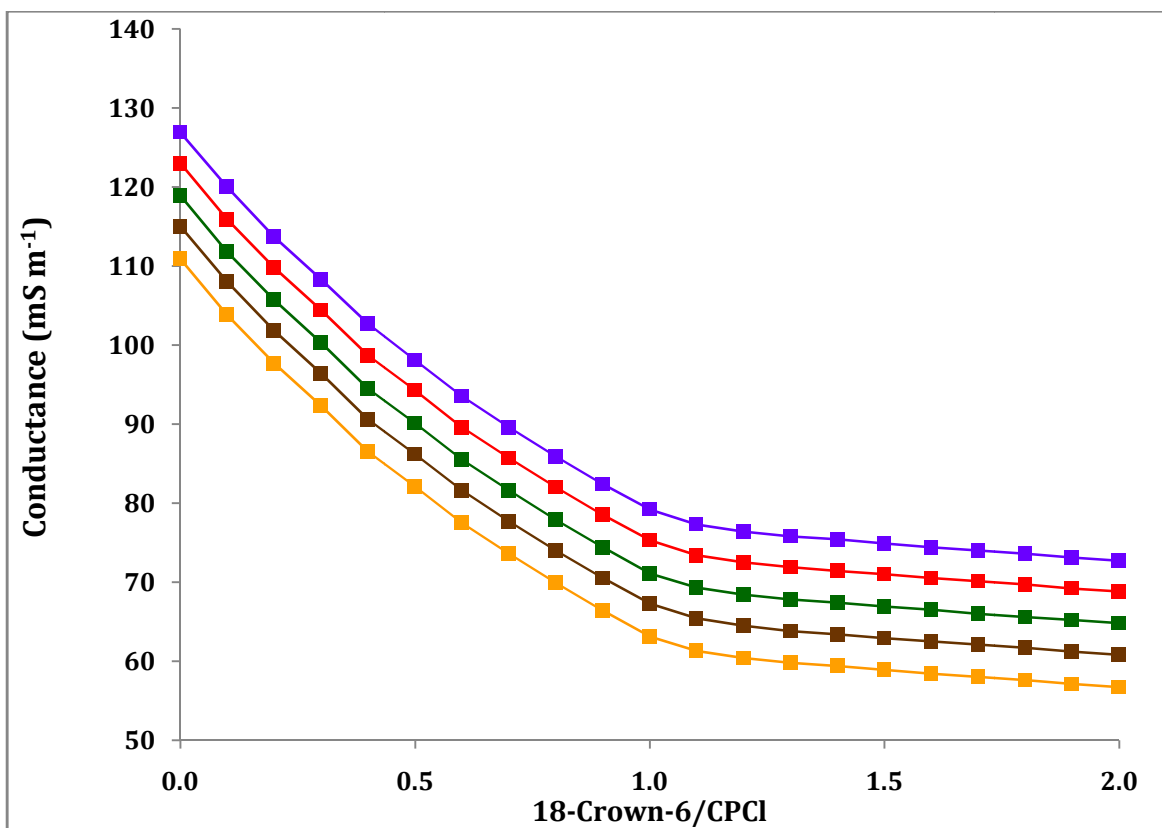


Figure 2. Variation of conductance of 18-crown-6/CPCI mole ratio at different temperatures (■ 293 K, ■ 298 K, ■ 303 K, ■ 308 K, ■ 313 K).

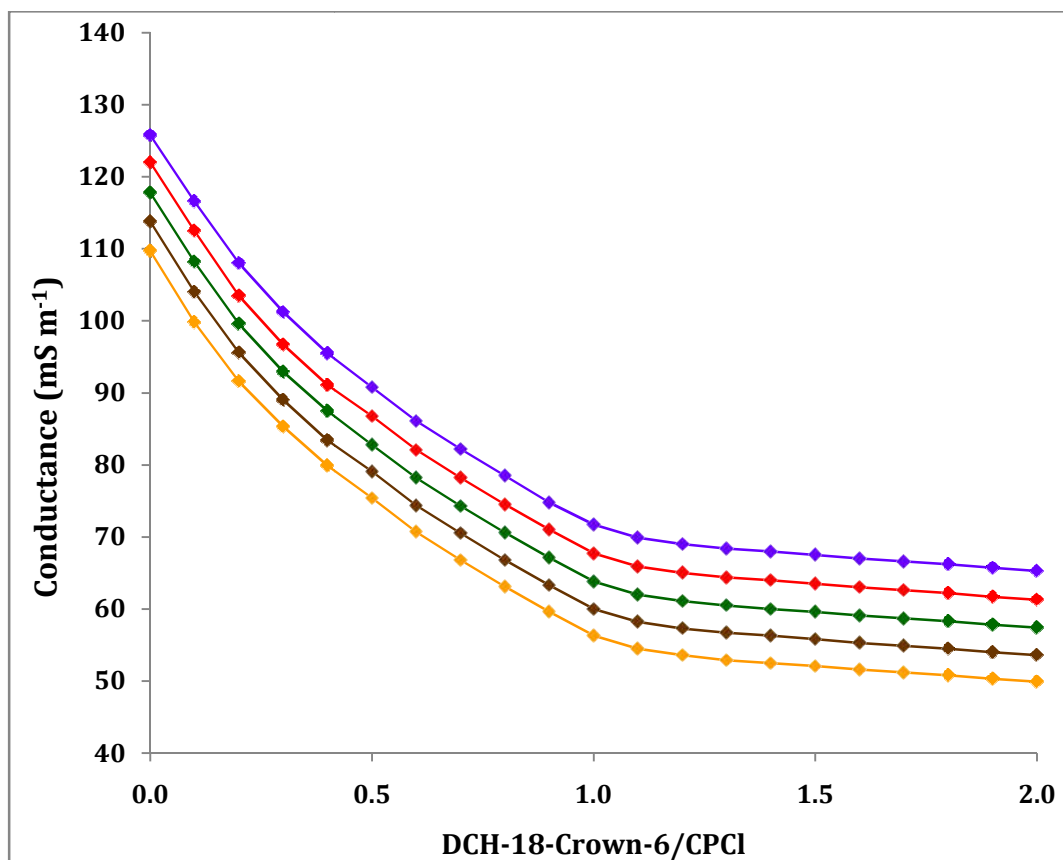


Figure 3. Variation of conductance of DCH-18-crown-6/CPCl mole ratio at different temperatures (\blacklozenge 293 K, \blacklozenge 298 K, \blacklozenge 303 K, \blacklozenge 308 K, \blacklozenge 313 K).

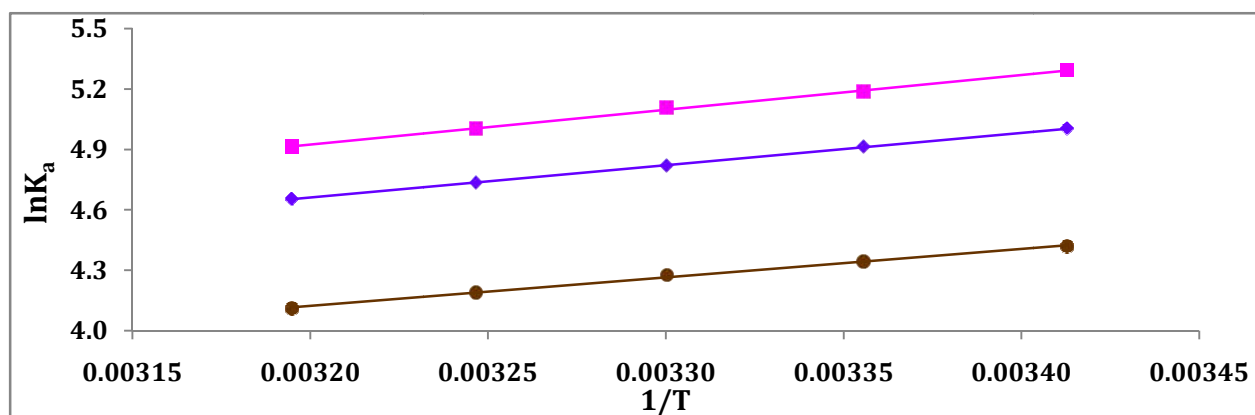


Figure 4. Plot of $\ln K_a$ vs $1/T$ for the interaction of CPCl with DB-18-C-6 (\bullet), 18-C-6 (\blacklozenge) and DCH-18-C-6 (\blacksquare).

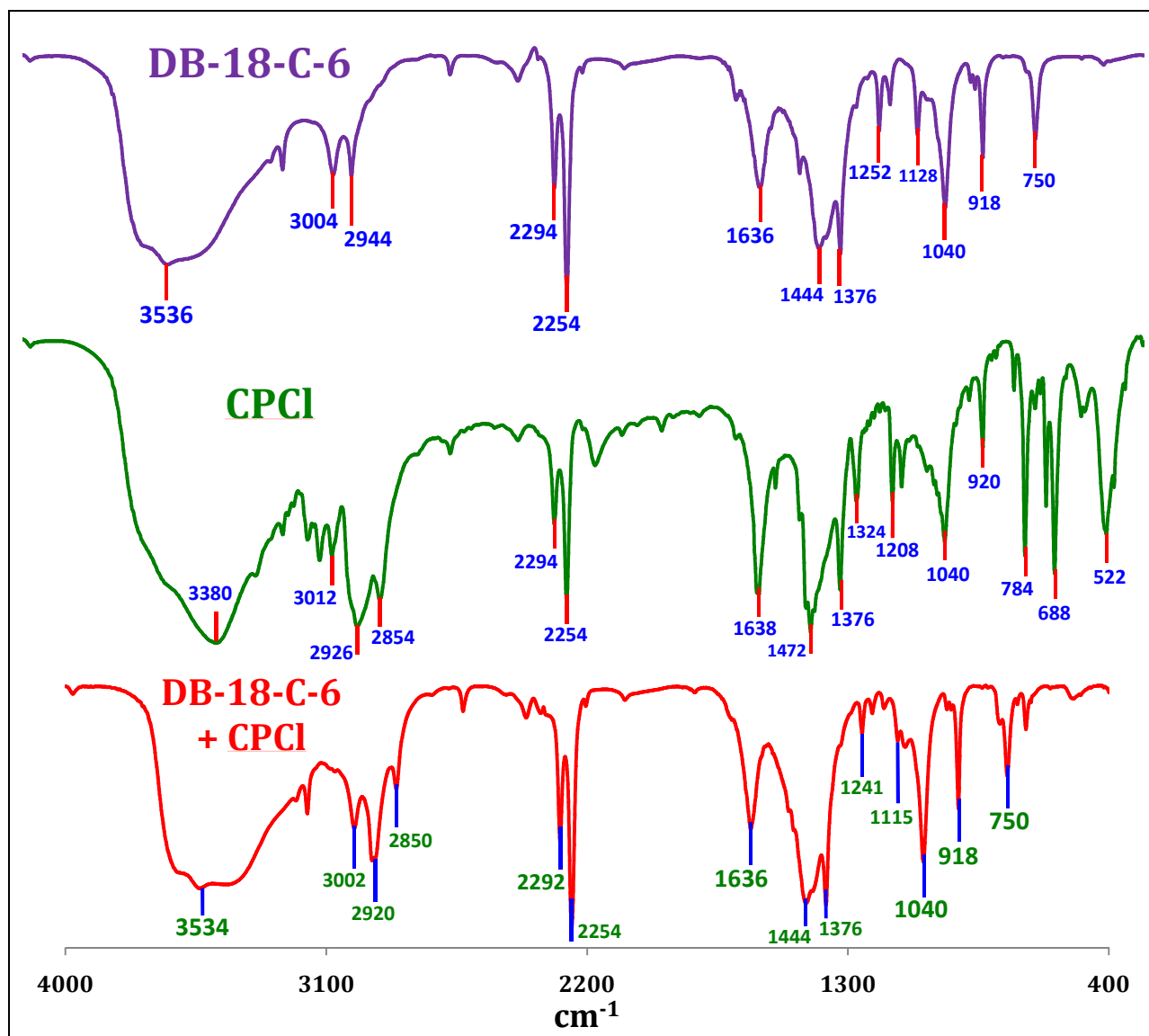


Figure 5. FTIR spectra of DB-18-C-6 (top), CPCI (middle) and complex (bottom).

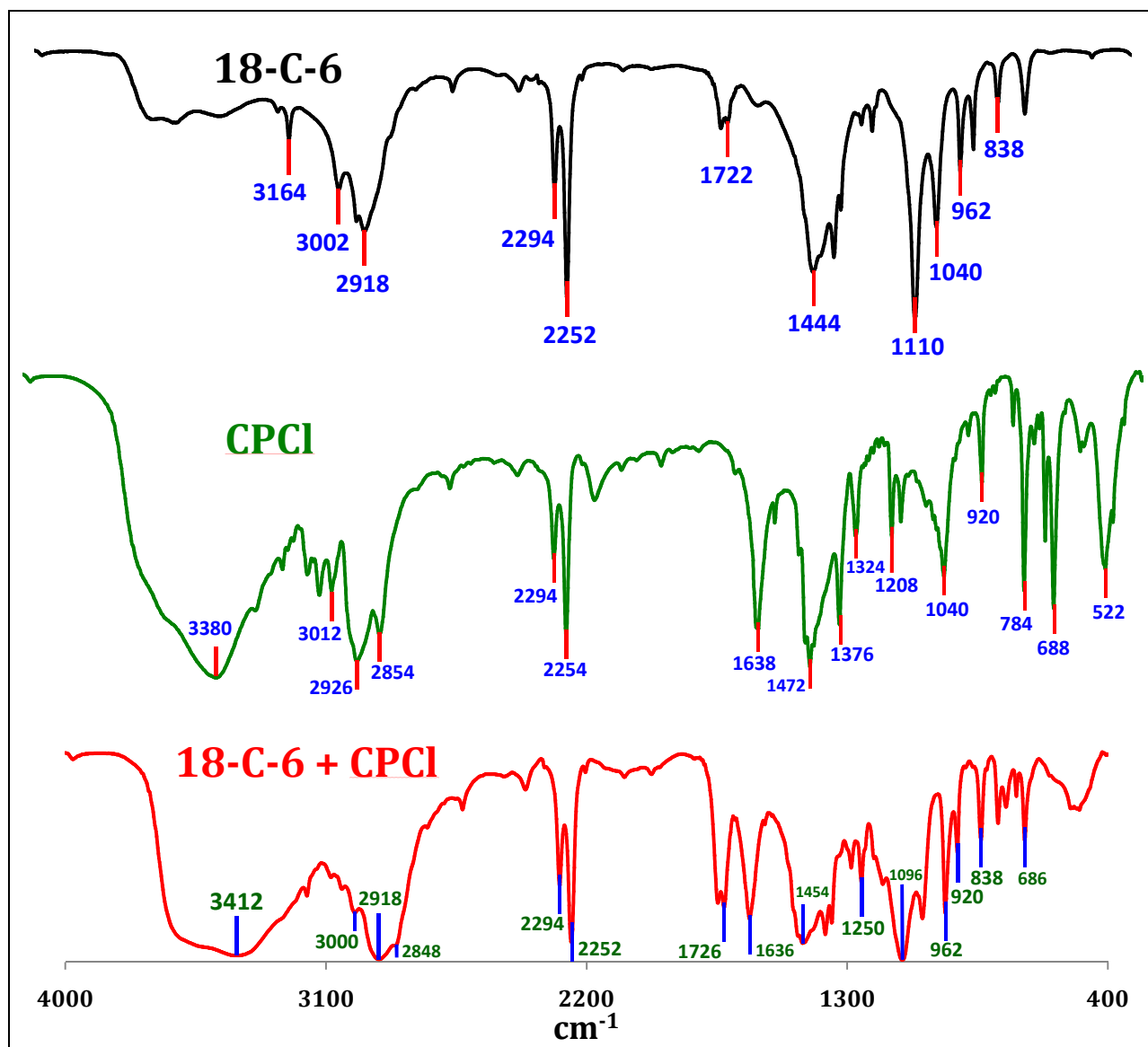


Figure 6. FTIR spectra of 18-C-6 (top), CPCI (middle) and complex (bottom).

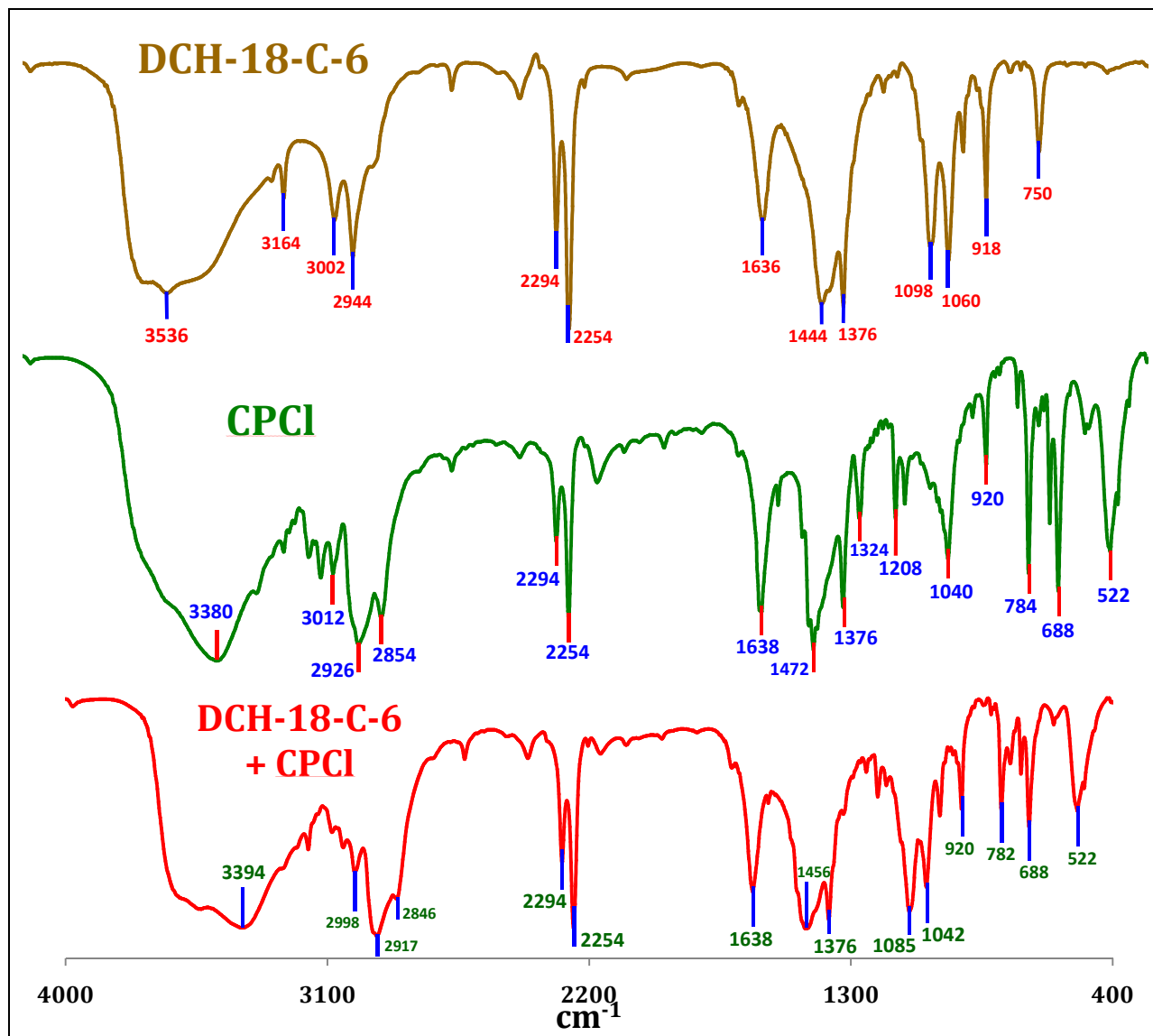


Figure 7. FTIR spectra of DCH-18-C-6 (top), CPCI (middle) and complex (bottom).

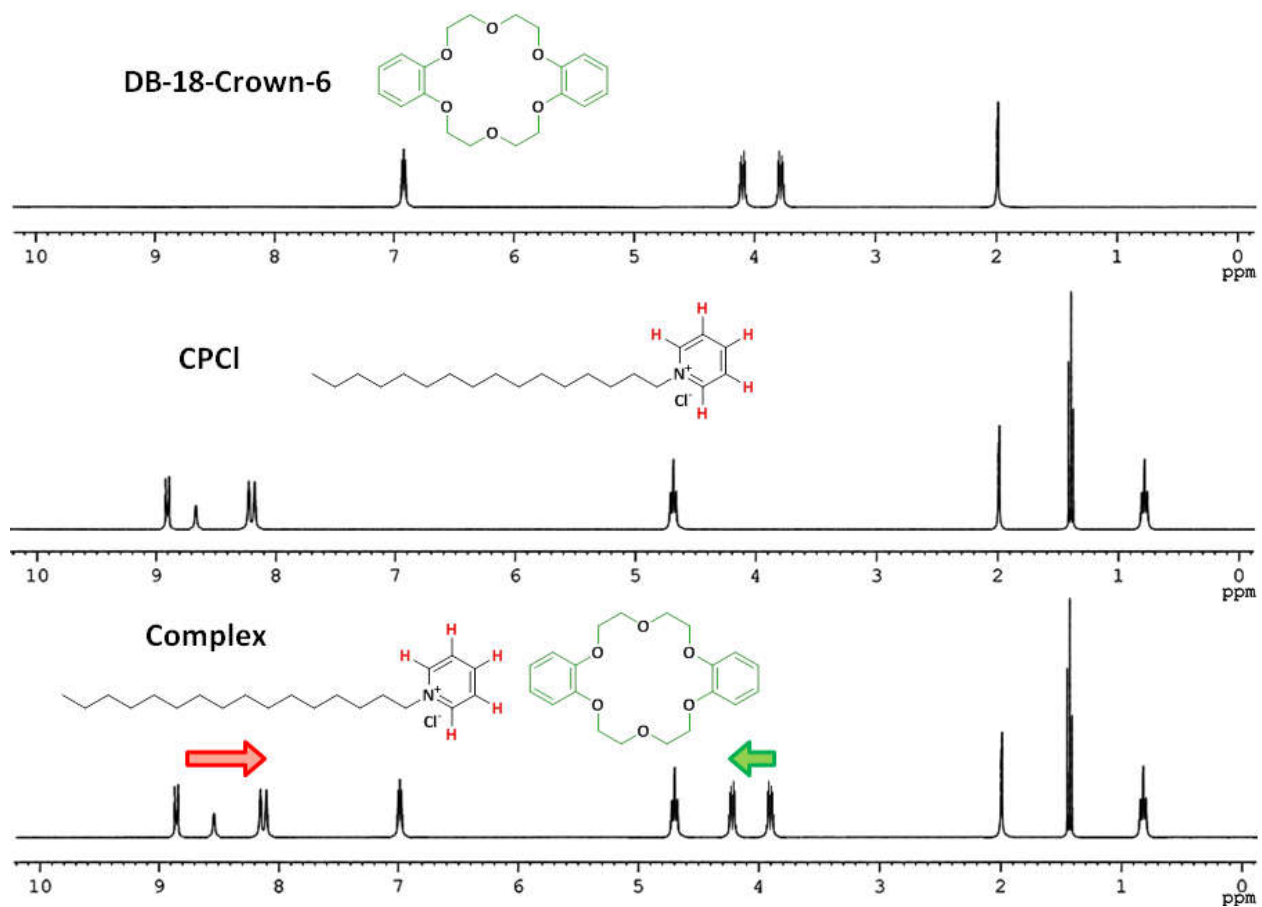


Figure 8. ^1H NMR spectra of DB-18-Crown-6, CPCl and complex in CD_3CN at 298.15 K.

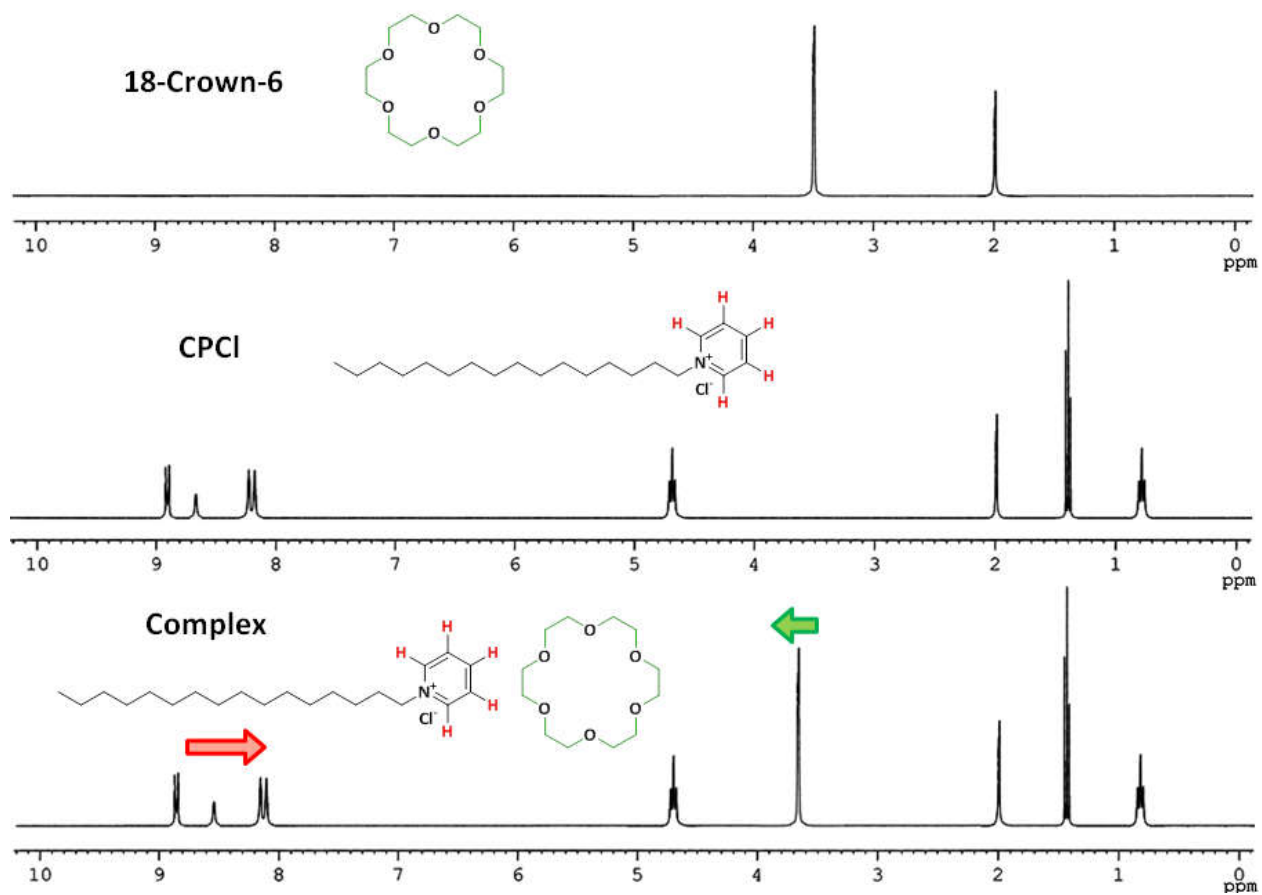


Figure 9. ^1H NMR spectra of 18-Crown-6, CPCI and complex in CD_3CN at 298.15 K.

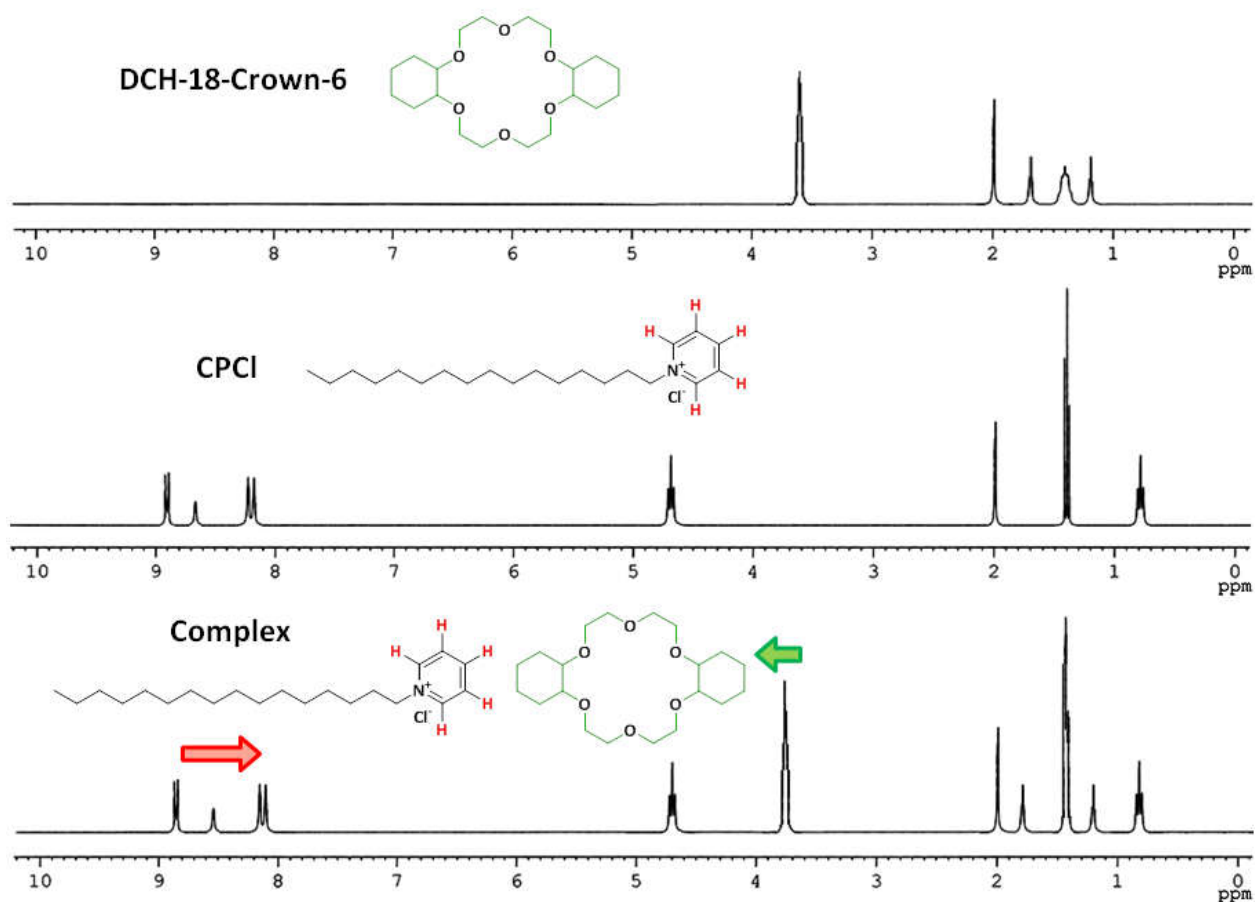
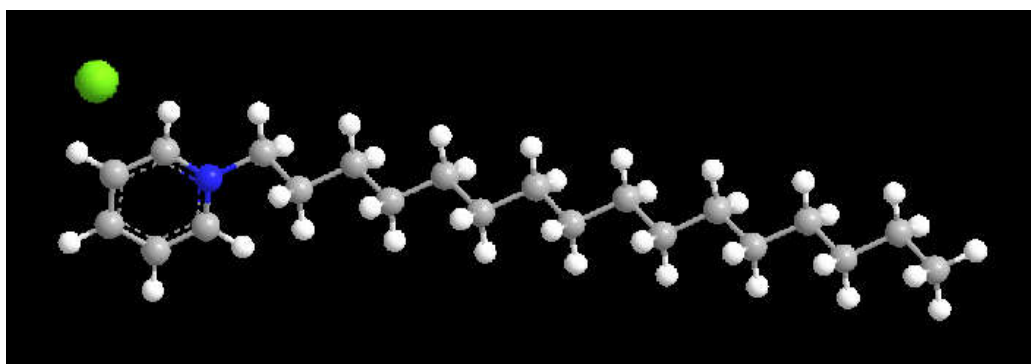
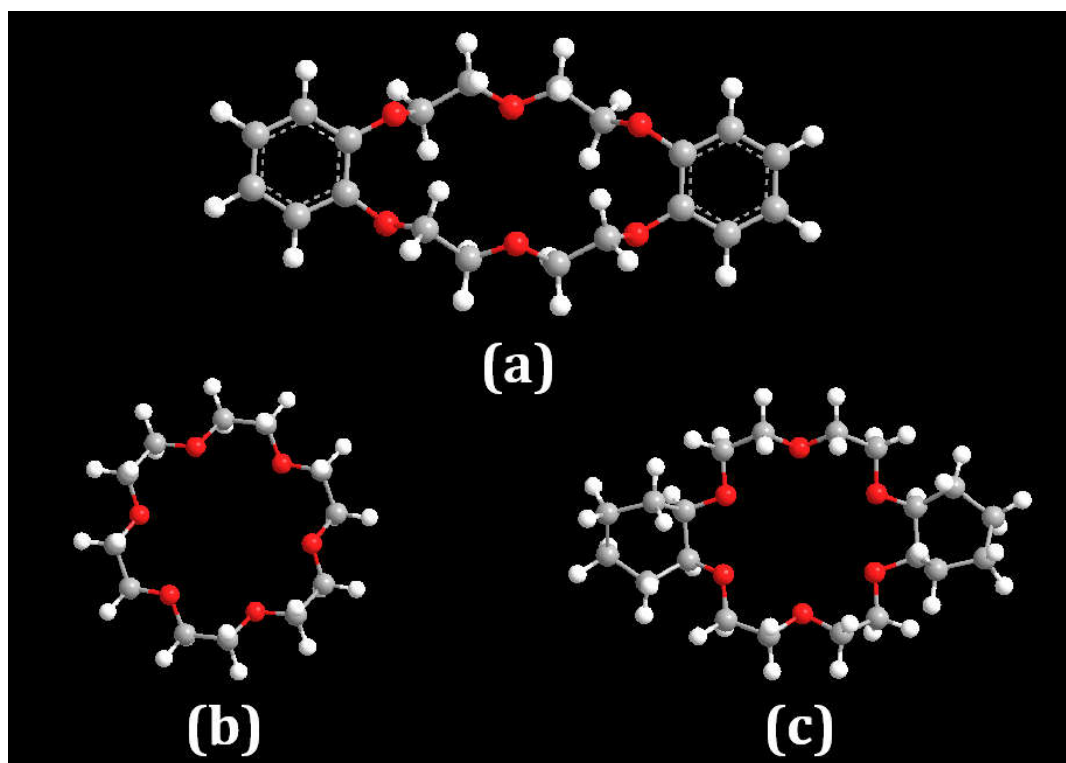


Figure 10. ^1H NMR spectra of DCH-18-Crown-6, CPCl and complex in CD_3CN at 298.15 K.

Schemes



Scheme 1. Molecular structure of cetylpyridinium chloride (CPCl).



Scheme 2. Molecular structure of (a) Dibenzo-18-crown-6 (DB-18-C-6), (b) 18-crown-6 (18-C-6) and (c) dicyclohexano-18-crown-6 (DCH-18-C-6).